Using inertial and magnetic sensors for hand tracking and rendering in wearable haptics

Tommaso Lisini Baldi[1,2], Mostafa Mohammadi [1,2], Stefano Scheggi [1], and Domenico Prattichizzo [1,2]

***Abstract*— In the last years, wearable haptic technologies became very promising since they provide the users with tactile force feedback via small and wearable interfaces. However, they have no position sensing thus additional technologies like motion capture systems or expensive gloves are required. Recently, low cost hand tracking systems based on RGB-D cameras have been developed, however they suffer from lighting conditions and occlusions. In this paper we present a sensing glove based on inertial and magnetic sensors for hand tracking which can be combined with cutaneous devices for the rendering of the force feedback, thus producing a wearable sensing/actuation system. The sensing glove does not suffer from occlusion problems, it is wearable and cost effective however, since the employed sensors use the magnetometer to compensate the drift, they are sensitive to variations in the magnetic field. This property makes it challenging to interface the sensing glove with wearable devices since their motors generate variations in the magnetic field. Preliminary experiments showed the effectiveness of using inertial and magnetic sensors for hand tracking. A comparison between using the glove with and without the haptic devices was presented in order to compare the tracking performance when cutaneous devices are used.**

I. INTRODUCTION

In the recent years, wearable haptic technologies have been very promising since they provide the users with tactile force feedback via small, lightweight and wearable devices [1], [2]. However, they have no position sensing; thus, additional technologies are required to detect the pose of these interfaces. Motion capture systems such as PhaseSpace or Vicon represent some expensive solutions, and require a structured environment. Similarly, grounded tracking systems (e.g., trakSTAR) are not as wearable/portable as the rendering devices.

Advancement in computer vision techniques made cameras an appealing solution for hand and human body tracking [3], [4]. Preliminary steps toward wearability in both sensing and actuation were made in [5] in which the authors presented a scenario where the human hand is tracked using a model based algorithm via an RGB-D camera, and haptic feedback is provided via wearable cutaneous devices. In the aforementioned application the camera is static in the environment. A step further in terms of sensing wearability was presented in [6] where the authors presented a wrist-worn device that recovers the full 3D pose of the user's hand using a technique similar to [3]. Image-based tracking algorithms are very promising since they do not require the user to wear additional equipments like gloves. However, computer vision techniques for hand tracking have several limitations: they are sensitive to lighting conditions, they suffer from occlusions of the hand, RGB-D cameras (e.g., Microsoft's Kinect or Asus Xtion) can not properly work in an outdoor environment, and since a grounded camera is needed, they are not completely portable/wearable.

Glove-based tracking systems represent a large group of sensing devices worn on the hand [7]. The former results in this area, datagloves, are mainly based on piezoresistive, fiberoptic, magnetic, and Hall-effect sensors. To name a few, in [8] a piezoresistive based dataglove was developed to measure flexion of fingers. A similar work, which also includes adduction-abduction measurement, is presented in [9]. Recently in [10] the authors presented a preliminary glove based on piezoresistive goniometer technology to reconstruct the whole hand posture in grasping tasks.

In spite of many benefits, the considered sensing gloves have some drawbacks such as adversity of calibration for individual subjects' hands and lack of absolute orientation of the hand. Emerging and rapid growing MEMS (Micro Electro-Mechanical Systems) sensor technology can represent a possible solution to these problems since they provide orientation estimation without the need of external actuators or cameras. The main drawback of IMU/MARG (Inertial Measurement Unit, Magnetic Angular Rate and Gravity) sensors is that they use magnetometer to compensate the drift of the gyroscope, and thus they are sensitive to variations in the magnetic field. Nevertheless, commercial tracking systems based on this technology are available and allow to accurately track the human body motion (with exception of the hands) in indoor as well as outdoor and unstructured environments [11]. Focusing on hand tracking, a sensing glove using dual-axis accelerometers was developed in [12] to recognize static postures for sign languages. The authors used 6 dual-axis accelerometers placed on the back of fingers. An improved version using triaxial accelerometers was presented in [13]. The system is able to detect simple gestures, but a limited number of joints can be measured independently and they cannot track all the human movements. A sensing glove instrumented with AHRS (Attitude and Heading Reference System) has been proposed in [14]. For each finger, the authors used 2 triaxial gyroscope accelerometer pairs placed on the proximal and intermediate phalanges and a triaxial magnetometer placed on the fingertip. In our opinion this work represent the most detailed and interesting work on

The research leading to these results has received funding from the European Union Seventh Framework Programme FP7/2007-2013 under grant agreement n. 601165 of the project "WEARHAP - WEARable HAPtics for humans and robots".

[1] Authors are with the Department of Information Engineering and Mathematics, University of Siena, 53100 Siena, Italy. {lisini, mohammadi, scheggi, prattichizzo}@diism.unisi.it

[2] Authors are with the Department of Advanced Robotics, Istituto Italiano di Tecnologia, Genova, 16163, Italy. {tommaso.lisini, mostafa.mohammadi, domenico.prattichizzo}@iit.it

using inertial and magnetic sensors for hand tracking.

In this work, we present a sensing glove based on IMU/MARG sensors which can be combined with cutaneous devices for the rendering of the force feedback, thus producing a wearable sensing/actuation system. To the best of our knowledge, this paper represents the first attempt to combine a sensing glove based on inertial and magnetic sensors with cutaneous devices. Using cutaneous devices introduces the following problems: (i) the sensors of the glove should be placed accordingly to the dimension and position of the cutaneous interfaces in order to not compromise the wearability of the system; (ii) the sensors employed in the glove are sensitive to variations in the magnetic field generated by the motors of the cutaneous devices.

In order to not compromise the wearability when the sensing glove is combined with the cutaneous devices, we decided to use a simplified kinematic model of the hand which requires a reduced number of sensors to detect the hand pose. Moreover, we took advantages from biomechanical constraints of the human hand that Cobos et al. [15] and Hrabia et al. [16] have deeply studied. We coupled the glove with an active wearable device [5] which provides force feedback in case of contact with a virtual object.

The rest of the paper is organized as follows. Section II presents the data fusion algorithm that estimates the orientation of a single IMU/MARG sensor. Section III describes the model of the hand and the algorithm used to track it. Section IV reports the results of experimental validations. Finally, in Section V conclusions are drawn and possible subjects of future research are outlined.

II. Orientation estimation of IMU/MARG sensors

In the proposed work, we tested and implemented three different algorithms for the orientation estimation of IMU/MARG sensors: (i) a gradient descent algorithm coupled with a complementary filter to fuse gyroscope, magnetometer and accelerometer data [17], (ii) a Gauss-Newton method with an Extended Kalman Filter (EKF) in a quaternion version [18], and (iii) a Gauss-Newton method combined with a complementary filter [19]. From our tests we decided to use the algorithm proposed in [19].

In this section we briefly review the data fusion algorithm that estimates the orientation of the sensor frame with respect to the world frame. The proposed algorithm uses quaternions to represents rotations. This choice avoids the *gimbal lock* problem (gimbal lock occurs because the map from Euler angles to rotations is not a covering map). In this way, we can easily rotate from a frame to another one without loss of precision due to the trigonometric functions.

At each time t, the gyroscope estimates the angular rates ${}^S\omega_x(t)$, ${}^S\omega_y(t)$ and ${}^S\omega_z(t)$ referred to the $x-$, $y-$ and $z-$axis of the sensor frame S. These values can be represented as a quaternion

$$ {}^S\boldsymbol{\omega}(t) = 0 + \boldsymbol{i}\,{}^S\omega_x(t) + \boldsymbol{j}\,{}^S\omega_y(t) + \boldsymbol{k}\,{}^S\omega_z(t) $$

assuming that the first component of ${}^S\boldsymbol{\omega}(t)$ is a real number. We consider the rate of change of orientation as a quaternion infinitesimal variation,

$$ {}^S\dot{\mathbf{g}}(t) = \frac{1}{2}\Big({}^S\mathbf{g}(t-\delta t) \otimes {}^S\boldsymbol{\omega}(t)\Big) \tag{1} $$

where ${}^S\mathbf{g}(t-\delta t)$ is the latest estimated quaternion, ${}^S\boldsymbol{\omega}(t) = [\ 0\ {}^S\omega_x(t)\ {}^S\omega_y(t)\ {}^S\omega_z(t)\ ]^T$ is the angular rate vector at the current time, $\otimes$ is the quaternion product, and δt is the sampling time.

Computing quaternions from accelerometer and magnetometer values is a bit more tricky. The idea behind the algorithm, which is based on the Gauss-Newton method, is to use the measurement of gravity and Earth's magnetic flux obtained from the IMU/MARG sensor in order to compute an adjusted measurements of rotation and to limit the effects of drifting in the orientation estimate due to the gyroscope integration.

Let ${}^S\mathbf{a}(t)$, ${}^S\mathbf{m}(t) \in \Re^{3\times 1}$ the accelerometer and magnetic components expressed in the sensor reference frame, and let

$$ {}^S\mathbf{z}(t) = \begin{bmatrix} {}^S\mathbf{a}(t) \\ {}^S\mathbf{m}(t) \end{bmatrix} \in \Re^{6\times 1}. $$

Similarly we assume the earth's reference vector

$$ {}^W\mathbf{z}(t) = \begin{bmatrix} 0 \\ 0 \\ 1 \\ {}^W\mathbf{m}(t) \end{bmatrix} \in \Re^{6\times 1}, $$

and the orientation estimation error

$$ \epsilon(t) = {}^W\mathbf{z}(t) - {}^W\mathbf{M}_S(t)\,{}^S\mathbf{z}(t) \tag{2} $$

where

$$ {}^W\mathbf{M}_S(t) = \begin{bmatrix} {}^W\mathbf{R}_S(t) & \mathbf{0} \\ \mathbf{0} & {}^W\mathbf{R}_S(t) \end{bmatrix} \in \Re^{6\times 6}, $$

and ${}^W\mathbf{R}_S(t) \in \mathbf{SO}(3)$ is the rotation matrix between the sensor frame S and the world frame W.

Suppose that we want to estimate ${}^W\mathbf{R}_S(t)$ (and consequently ${}^W\mathbf{M}_S(t)$) in Eq. (2) by using an optimization algorithm like the Gauss-Newton optimization method. Let $\mathbf{q}(t)$ be the quaternion representation of the rotation matrix ${}^W\mathbf{R}_S(t)$. If we write a single step of the Gauss-Newton optimization method in a quaternion form we obtain

$$ \mathbf{q}_{k+1}(t) = \mathbf{q}_k(t) - \mathbf{J}_k^{\dagger}(t)\epsilon(t) \tag{3} $$

where

$$ \mathbf{J}_k^{\dagger}(t) = (\mathbf{J}_k^T(t)\mathbf{J}_k(t))^{-1}\mathbf{J}_k^T(t), $$

the subscript k represents the iteration of the optimization algorithm and $\mathbf{J}_k(t)$ is the Jacobian of the error $\epsilon(t)$ reported in Eq. (2). As suggested in [17], [19], we provided a compensation for magnetic distortion using the latest computed quaternion.

The second part of the algorithm fuses the quaternion estimated from the accelerometer and magnetometer components (see Eq. (3)) with the quaternion estimated from the gyroscope. This operation is provided by a very simple filter, known as complementary filter. The filter uses two different gain factors whose sum is 1, chosen in order to reduce the noise of each component. The gyroscope quaternion $\mathbf{g}(t)$ is fused with the quaternion $\mathbf{q}(t)$ computed by the Gauss-Newton method. The resulting quaternion $\mathbf{r}(t)$ is obtained as,

$$ \mathbf{r}(t) = \alpha\mathbf{g}(t) + (1-\alpha)\mathbf{q}(t) $$

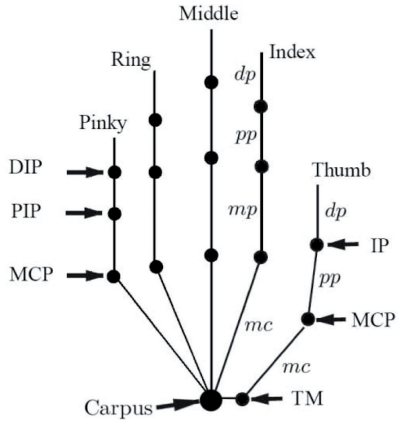

Fig. 1. 24-DoFs kinematic model of the human hand.

being $0 < \alpha < 1, \alpha \in \Re$ the gain of the complementary filter and

$$\mathbf{g}(t) = \mathbf{r}(t - \delta t) + \dot{\mathbf{g}}(t)\ \delta t$$

where $\dot{\mathbf{g}}(t)$ is computed according to Eq. (1). It is worth noting that $\mathbf{g}(t)$ is initialized as $\mathbf{g}(0) = [1\ 0\ 0\ 0]^T$. Please refer to [19] for more information about the performance of the proposed algorithm.

Concerning the calibration of the sensor, we used three different approaches to calibrate the accelerometer, the gyroscope and the magnetometer. The fundamental principle of the triaxial accelerometer calibration is that the sum of the outputs is equal to the gravity vector when the accelerometer is stationary, thanks to this assumption we can adjust the bias and the scale factor of the accelerometer. For the gyroscope, we estimated its bias. Finally, we performed the calibration of the magnetometer using the algorithm described in [20].

III. Tracking hand articulations based on IMU/MARG sensors

In what follows we present the simplified kinematic model of the hand, and we describe the design of the sensing glove as well as the proposed hand tracking algorithm using IMU/MARG sensors.

A. Hand modeling

We used a simplified kinematic structure of the hand, assuming universal joints (two intersecting, orthogonal revolute joints) and planar kinematic chains for the fingers. We did not model joint axis movements.

Referring to [21], we assumed that each finger has the metacarpal (MC) bone fixed with respect to the hand frame, and features four degrees of freedom (DoFs). The trapeziometacarpal (TM) joint of the thumb as well as the metacarpophalangeal (MCP) joint of the index, middle, ring and pinky fingers have 2 DoFs each (one for adduction-abduction and another for flexion/extension). The MCP and interphalangeal (IP) joints of the thumb, as well as the proximal interphalangeal (PIP) and distal interphalangeal (DIP) joints of the other fingers have 1 DoF each. The position and orientation of the TM joint with respect to the wirst has been numerically tuned. Fig. 1 shows the model of the hand used in this work. The kinematics of each finger is modeled using four parameters encoding angles, two for the base of the finger and two for the remaining joints. The global orientation is parameterized using the redundant representation of quaternions. The resulting parameterization encodes a 24-DoFs hand model with a representation of 24 parameters.

The human hand is extremely articulated, however the fingers' movements are constrained to a specific range due to dynamic (intra-finger and inter-finger constraints) and static constraints (the limits of fingers' motions as a result of hand anatomy). Intra-finger constraints relate the joints of the same finger. Inter-finger constraints refer to the ones imposed on the joints values between different fingers. In [15] the authors identified an intra-finger constraint between the DIP and the PIP joint angles ($\theta_{DIP} \simeq 2/3\ \theta_{PIP}$), for each finger with the exception of the thumb. Recently, in [16] the authors performed additional tests starting from the results presented in [15] and they found the following relationship for the index, middle, ring and pinky fingers,

$$\theta_{DIP} \simeq 0.88\ \theta_{PIP} \tag{4}$$

and for the thumb

$$\theta_{IP} \simeq 0.77\ \theta_{MCP}. \tag{5}$$

Additionally, the authors found that neither the hand orientation or pose nor the used hand (left/right) have an influence on the linear relationship between the two upper finger joint angles. Although the authors presented a linear relationship between the IP and the MCP joint angles of the thumb (see Eq. (5)), they recommended to use 3 sensors on the thumb for high precision hand model. By using the constraints defined in Eq. (4), the proposed hand model can be parametrized by 20 parameters.

Static constraints on the values of each joint are based on anatomical studies, see [15], [22] and the references therein. For example, fingers (with exception of the thumb) have an active flexion range of the MCP joint of 90 deg and an extension of about 40 deg. The abduction-adduction range is about 50 deg. The PIP joint actively flex more than 90 deg and the DIP joints slightly less than 90 deg. Table I reports the static constraints used in this work, in accordance with [15].

B. Sensing glove design and hand tracking

We designed a sensing glove which could be combined with cutaneous devices. The cutaneous devices considered herein are assumed to be rigidly attached to the intermediate or distal phalanges of the fingers [1], [2]. Following the guidelines defined in the previous section, we designed a sensing glove made by 12 sensors (1 sensor for the palm, 3 sensors for the thumb and 2 sensors for each of the remaining fingers). For the index, middle, ring, and pinky fingers, we placed the sensors on the intermediate and proximal phalanges and we exploited the relationship between the upper finger joints DIP and PIP, as previously described. Since the considered cutaneous devices are rigidly attached to the intermediate phalanges of the fingers, we placed the

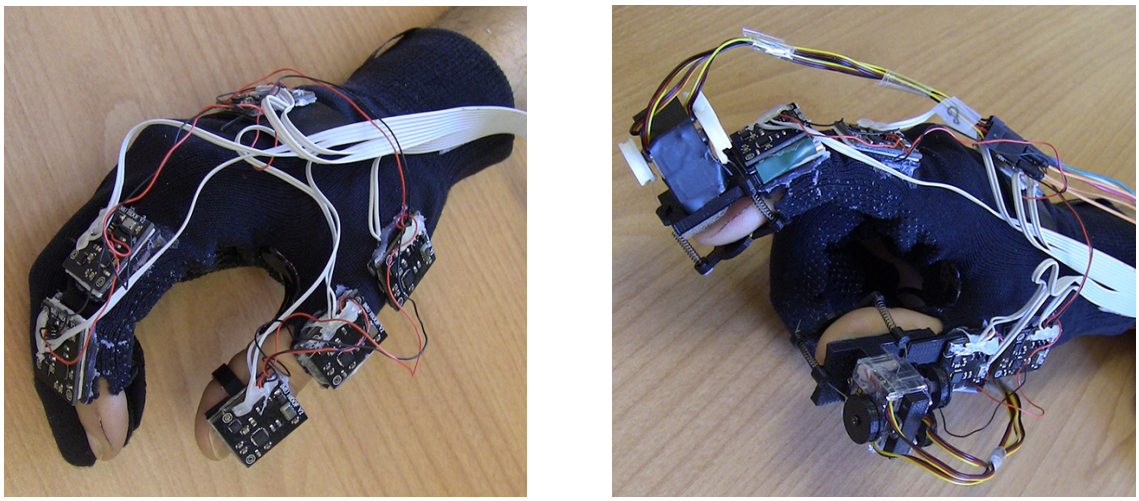

(a) (b)

Fig. 2. The proposed prototype was designed to be combined with cutaneous devices. The preliminary version estimates the orientation of the palm and the joint values of the thumb and the index fingers. It is made by 6 sensor units (1 for the palm, 3 for the thumb and 2 for the index) when used stand-alone (a) and 5 sensor units when coupled with the wearable haptic devices (b).

TABLE I
STATIC CONSTRAINTS OF THE FINGERS.

Finger	Joint	Flexion (deg)	Extension (deg)	Abduction/adduction (deg)
Thumb	TM	90	15	60
	MCP	80	0	0
	IP	80	10	0
Index	MCP	90	40	60
	PIP	110	0	0
	DIP	90	5	0
Middle	MCP	90	40	45
	PIP	110	0	0
	DIP	90	5	0
Ring	MCP	90	40	45
	PIP	120	0	0
	DIP	90	5	0
Pinky	MCP	90	40	50
	PIP	135	0	0
	DIP	90	5	0

IMU/MARG sensors on the intermediate phalanx instead of the distal one. In this way, when the wearable devices are used, we just need to move the sensor on the haptic interface. For the thumb, when the sensing glove is used stand-alone, we placed a sensor on each phalanx and we did not impose any biomechanical constraint. When it is combined with the cutaneous devices, we removed the sensor from the distal phalanx and we moved the sensor from the intermediate phalanx to the device. In this case, we used Eq. (5) to estimate the IP joint value of the thumb.

The tracking algorithm requires an initial calibration phase which is composed by three steps. In the first two steps, the user is asked to place the hand in an initial *a priori* hand pose. We assume as initial pose the hand configuration in which all joint values are approximately zero. The user is asked to place the hand on a flat surface and to not move the hand. In the first calibration step, each IMU/MARG sensor uses 200 samples to estimate its gyroscope offset. In the second step, for each hand joint we compute the offset quaternion. In the third calibration step, we used an approach similar to [11] to estimates the links lengths by using a priori knowledge about the distance between two points in the kinematic chain. The user is asked to touch in turn the fingertip of the thumb with the fingertip of the other fingers and moving the fingers without applying forces to the finger pads in order to not violate the constraint in Eq. (4). Since the distance between the finger pads is zero for each pose, we can use the kinematic chain to improve the estimation of the links lengths.

In what follows, we report the joint estimation for the index (the same approach can be used for the middle, ring and pinky finger) and the thumb. Let us consider the index finger and let ${}^{W}\mathbf{q}_0(t)$, ${}^{W}\mathbf{q}_P(t)$, ${}^{W}\mathbf{q}_I(t)$, the quaternions that define the orientation of the frames associated to the palm and the phalanges (proximal and intermediate) with respect to the global reference frame W, respectively. Let ${}^{0}\hat{\mathbf{q}}_P$, ${}^{P}\hat{\mathbf{q}}_I$ be the offset quaternions estimated during the calibration phase between the proximal phalanx and the palm and between the intermediate phalanx and the proximal one, respectively. The orientation of the proximal phalanx with respect to the palm is computed as ${}^{0}\mathbf{q}_P(t) = {}^{0}\mathbf{q}_W(t) \otimes {}^{W}\mathbf{q}_P(t)$, being ${}^{0}\mathbf{q}_W(t)$ the conjugate quaternion of ${}^{W}\mathbf{q}_0(t)$. Then, the quaternion which describes the rotation of the proximal phalanx with respect to the initial configuration is,

$$\mathbf{q}_P(t) = {}^{P}\hat{\mathbf{q}}_0 \otimes {}^{0}\mathbf{q}_P(t). \quad (6)$$

The orientation described by the quaternion $\mathbf{q}_P(t)$ can be converted in the Euler angles representation and used to compute the flexion and abduction-adduction values of the MCP joint. Similarly, the orientation of the intermediate phalanx with respect to the proximal one is computed as

$$\mathbf{q}_I(t) = {}^{I}\hat{\mathbf{q}}_P \otimes {}^{P}\mathbf{q}_W(t) \otimes {}^{W}\mathbf{q}_I(t). \quad (7)$$

Then, the Euler angles representation is used to compute the value of the PIP joint. Finally, the DIP joint angle is

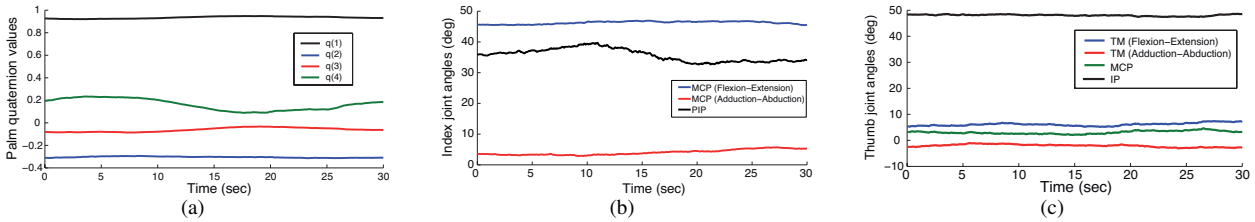

(a) (b) (c)

Fig. 3. Experiment 1: the user was asked to gently grasp a light object and move his/her hand along an eight-like path maintaining the initial palm orientation. (a) Quaternion values of the palm. (c) Joint angles of the index finger. (d) Joint angles of the thumb.

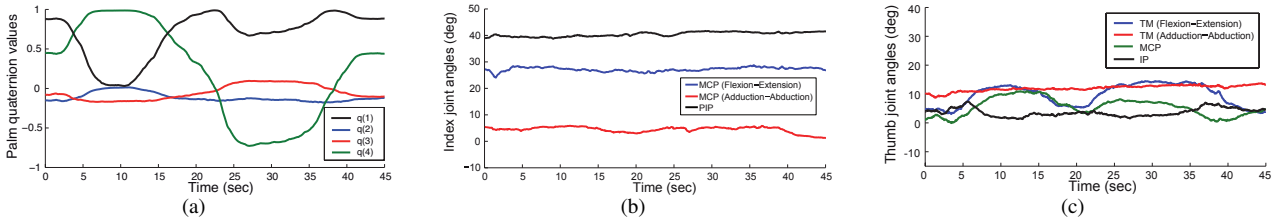

(a) (b) (c)

Fig. 4. Experiment 1: the user was asked to gently grasp a light object and move his/her hand along an eight-like path following the path orientation. (a) Quaternion values of the palm. (b) Joint angles of the index finger. (c) Joint angles of the thumb.

computed from the estimated values of the PIP joint, as described in Eq. (4).

For the thumb, we used 3 sensors placed on each phalanx of the finger. Differently form the index finger, a third sensor is used on the distal phalanx when the glove is used without the cutaneous device. Thus, it is necessary to estimate the quaternion between the distal and the intermediate phalanx instead of using the biomechanical constraint proposed in Eq. (5). For the estimation of the joint values of the thumb, we used the approach previously described for the index. In order to avoid unnatural finger positions, we used the set of angles ranges reported in Table I.

In this work, we built a preliminary prototype which estimates the orientation of the palm and the joint values of the thumb and the index. Although preliminary, the proposed device shows all the capabilities of the proposed approach since all the fingers except the thumb share the same kinematic structure, thus the position of the sensors on the glove and the estimation of the joint values is the same for the index, medium, ring and pinky finger. The sensing glove is composed by 6 IMU/MARG modules and an Arduino nano with an ATmega328 microcontroller. Each IMU/MARG board contains a triaxial accelerometer/gyroscope (InvenSense MPU6050) and a triaxial magnetoresistor (Honeywell HMC5883L). These boards are placed on the back of the fingers and on the back of the palm (see Fig. 2). Arduino collects the raw data from the IMU/MARG boards and send them to an external PC through a 57600 bps serial connection which computes all the mathematical operations. The wearable devices consist of a static part placed over the finger nail and a mobile platform which applies the requested stimuli to the fingertip [1], [23]. Three springs are placed between the mobile platform and the static part and keep the platform horizontally aligned with the rest of the device. Three servo-motors (HS-5035HD Digital Ultra Nano servo) control the length of the three wires connecting the mobile platform to the static platform, allowing to apply the requested force at the user's fingertip.

Since IMU/MARG sensors use the magnetometer to compensate the drift of the gyroscope, they are sensitive to local variations in the magnetic field. To operate these sensors near a static object that has a magnetic field, it is necessary to calibrate the magnetometer in the exact position where it will be used later on (see Sect. II). In this case the magnetic disturbance can be treated like an offset. However, this step does not completely solve situations where the magnetic field changes dynamically, e. g. when cutaneous devices are used and the user moves her/his fingers the devices dynamically disturb the local earth magnetic field.

IV. Experimental validation

In order to show robustness, dynamic performance, precision, repeatability, and compatibility with wearable haptic devices, three different experiments have been performed.

The first experiment aimed to show the robustness of the system. We asked subjects to gently grasp a light object (in order to not violate the biomechanical constraints of the hand), and move their hand along an eight-like path, once keeping their palm initial orientation, and once following the path direction. The length of the path is about 90 cm. The position and orientation of palm is precisely recorded using Vicon tracking system. Joint angles of the fingers (see Sect. III-A) along with palm orientation are obtained using the proposed sensing glove. A typical result for an eight-like path is depicted in Fig. 3 and Fig. 4 for fixed, and variable palm orientation respectively. Palm orientation is shown in Fig. 3 (a) using quaternion values. Joints angles of index, and thumb fingers are illustrated in Fig. 3 (b)-(c), respectively. As shown, the joint angles do not change more than 2.5 deg. Fig. 4 (a) presents the quaternion values of palm, which follows the path direction. The identified hand gesture maintains and joint angles of fingers (see Fig. 4 (b)-(c)) do not vary more than 5 deg from their initial

values. The results of the experiment show that the identified hand configuration does not change too much during the hand motion. Variation in hand configuration are mainly due to: magnetic field of electrical equipment around, simplified kinematic hand model and subject's tremor.

The target of the second experiment is to show the dynamic performance and system output reliability in fingertips positioning. To this goal, we asked subjects to do flexion-extension, and adduction-abduction motions with their fingers several times. The ground truth values were obtained using an Omega3 haptic device (Force Dimension). The positions of fingertips are obtained by computing the forward kinematic of the hand. Typical results for index finger movements (flexion-extension and adduction-abduction) are depicted in Fig. 5. Vertical displacement of the index fingertip is shown in Fig. 5(a) for flexion-extension movement, while Fig. 5(b) depicts the lateral displacement of the index fingertip in adduction-abduction movement. The results show that the system has a high repeatability. Moreover, error of fingertip positioning is less than 2 mm in flexion-extension movement and 3 mm in adduction-abduction movement, subject to an appropriate estimation of link lengths.

In the last experiment, we evaluated the compatibility of the proposed glove with wearable rendering haptic devices. In this experiment subjects were asked to gently grasp a light object and freely rotate their hand without changing the grasp configuration. They repeated this task several times. This scenario has been performed in three deferent modes: without wearable rendering devices, with switched-off devices, and with switched-on devices (in this case the devices exerted the maximum force). Typical results for free rotations of the palm are shown in Figs. 6-8, respectively. This experiment revealed that the disturbing effect, due to the presence of magnetic materials very close to sensors, is not negligible. We observed about 10 deg diversion from initial values of joint angles for joints close to the magnetic parts. It is noticeable that there is not significant difference between the presence of a switched-off and a switched-on device, mainly because this kind of haptic interfaces utilize low current motors.

V. Conclusion and future work

In this paper we presented a sensing glove based on IMU/MARG sensors. The glove has been designed to find a trade off between tracking precision and wearability/portability of the system. Additional constraints in the design of the glove were generated by the fact that it should be combined with cutaneous devices which provide haptic feedback on the fingertips. Using the sensing glove with wearable haptic devices forced us to reduce the number of sensor units on the glove. Moreover, since IMU/MARG sensors are sensitive to changes in the magnetic field, placing these sensors close to motors represented a challenge.

In future works, we will design a more compact electronic system. Furthermore, more advanced algorithms [24] will be evaluated to increase the precision of the system, especially in the presence of dynamic disturbances in the magnetic field generated by wearable haptic devices.

References

[1] D. Prattichizzo, F. Chinello, C. Pacchierotti, and M. Malvezzi. Towards wearability in fingertip haptics: a 3-dof wearable device for cutaneous force feedback. *IEEE Trans. on Haptics*, 6(4):506–516, 2013.

[2] K. Minamizawa, S. Fukamachi, H. Kajimoto, N. Kawakami, and S. Tachi. Gravity grabber: wearable haptic display to present virtual mass sensation. In *Proc. ACM Special Interest Group on Computer Graphics and Interactive Techniques Conference (SIGGRAPH)*, page 8, 2007.

[3] I. Oikonomidis, N. Kyriazis, and A. Argyros. Efficient model-based 3d tracking of hand articulations using kinect. In *Proc. British Machine Vision Cconference (BMVC)*, pages 101.1–101.11, 2011.

[4] C. Qian, X. Sun, Y. Wei, X. Tang, and J. Sun. Realtime and robust hand tracking from depth. In *Proc. IEEE Conf. on Computer Vision and Pattern Recognition (CVPR)*, 2014.

[5] L. Meli, S. Scheggi, C. Pacchierotti, and D. Prattichizzo. Wearable haptics and hand tracking via an rgb-d camera for immersive tactile experiences. In *Proc. ACM Special Interest Group on Computer Graphics and Interactive Techniques Conference (SIGGRAPH)*, page 56, Vancouver, Canada, 2014.

[6] D. Kim, O. Hilliges, S. Izadi, A.D. Butler, J. Chen, I. Oikonomidis, and P. Olivier. Digits: freehand 3d interactions anywhere using a wrist-worn gloveless sensor. In *Proc. Symp. on User Interface Software and Technology*, pages 167–176, 2012.

[7] L. Dipietro, A. M. Sabatini, and P. Dario. A survey of glove-based systems and their applications. *IEEE Trans. on Systems, Man, and Cybernetics, Part C: Applications and Reviews*, 38(4):461–482, 2008.

[8] L. K. Simone, N. Sundarrajan, X. Luo, Y. Jia, and D. G. Kamper. A low cost instrumented glove for extended monitoring and functional hand assessment. *Journal of neuroscience methods*, 160(2):335–348, 2007.

[9] R. Gentner and J. Classen. Development and evaluation of a low-cost sensor glove for assessment of human finger movements in neurophysiological settings. *Journal of neuroscience methods*, 178(1):138–147, 2009.

[10] M. Bianchi, N. Carbonaro, E. Battaglia, F. Lorussi, A. Bicchi, D. De Rossi, and A. Tognetti. Exploiting hand kinematic synergies and wearable under-sensing for hand functional grasp recognition. In *Proc. Int. Conf. on Wireless Mobile Communication and Healthcare*, 2014.

[11] D. Roetenberg, H. Luinge, and P. Slycke. Xsens mvn: full 6dof human motion tracking using miniature inertial sensors. Technical report, Xsens Motion Technologies BV, 2009.

[12] J. L. Hernandez-Rebollar, N. Kyriakopoulos, and R. W. Lindeman. The acceleglove: a whole-hand input device for virtual reality. In *Proc. ACM Special Interest Group on Computer Graphics and Interactive Techniques Conference*, pages 259–259, 2002.

[13] Y. S. Kim, B. S. Soh, and S. Lee. A new wearable input device: Scurry. *IEEE Trans. on Industrial Electronics*, 52(6):1490–1499, 2005.

[14] H. G. Kortier, V. I. Sluiter, D. Roetenberg, and P. H. Veltink. Assessment of hand kinematics using inertial and magnetic sensors. *Journal of Neuroengineering and Rehabilitation*, 11(1):70, 2014.

[15] S. Cobos, M. Ferre, M. A. Sánchez-Urán, and J. Ortego. Constraints for realistic hand manipulation. *Proc. Presence*, pages 369–370, 2007.

[16] C. Hrabia, K. Wolf, and M. Wilhelm. Whole hand modeling using 8 wearable sensors: biomechanics for hand pose prediction. In *Proc. ACM Int. Conf. on Augmented Human*, pages 21–28, 2013.

[17] S. Madgwick, A. Harrison, and R. Vaidyanathan. Estimation of imu and marg orientation using a gradient descent algorithm. In *Proc. IEEE Int. Conf. on Rehabilitation Robotics*, pages 1–7, 2011.

[18] J. L. Marins, X. Yun, E. R. Bachmann, R. McGhee, and M. J. Zyda. An extended kalman filter for quaternion-based orientation estimation using marg sensors. In *Proc. IEEE/RSJ Int. Conf. on Intelligent Robots and Systems*, pages 2003–2011, 2001.

[19] D. Comotti. Orientation estimation based on gauss-newton method and implementation of a quaternion complementary filter. Technical report, 2011.

[20] J. Merayo, P. Brauer, F. Primdahl, J. Petersen, and O. Nielsen. Scalar calibration of vector magnetometers. *Measurement Science and Technology*, 11(2):120, 2000.

[21] S. Mulatto, A. Formaglio, M. Malvezzi, and D. Prattichizzo. Using postural synergies to animate a low-dimensional hand avatar in haptic simulation. *IEEE Trans. on Haptics*, 6(1):106–116, 2013.

[22] I. M. Bullock, J. Borràs, and A. M. Dollar. Assessing assumptions in kinematic hand models: a review. In *Proc. IEEE Conf. on Biomedical Robotics and Biomechatronics*, pages 139–146, 2012.

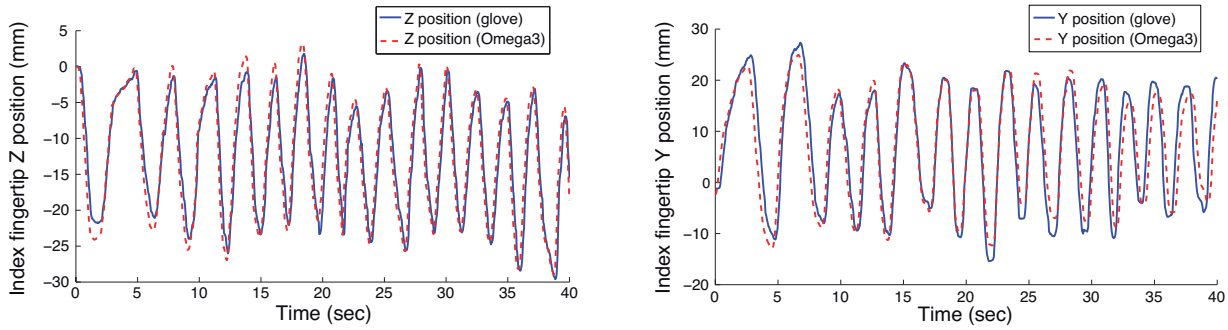

(a) (b)

Fig. 5. Experiment 2: position estimation of the index fingertip. (a) Vertical displacement of the index fingertip in flexion-extension motion. (b) Lateral displacement of the index fingertip in adduction-abduction motion. The dashed red curves show the displacement of the fingertip provided by Omega3 haptic device while the solid blue curves represent the estimation obtained by the sensing glove.

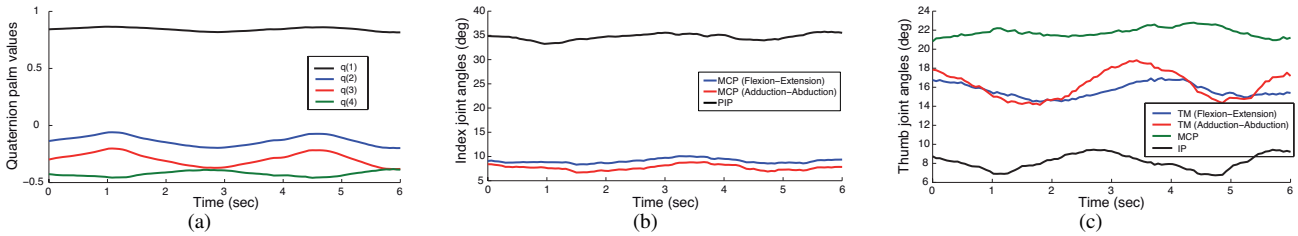

(a) (b) (c)

Fig. 6. Experiment 3: the user was asked to gently grasp a light object and freely rotate the palm maintaining the grasp configuration without wearable haptic devices. (a) Quaternion of the palm during the motion. (b) Joint angles of the index finger. (c) Joint angles of the thumb.

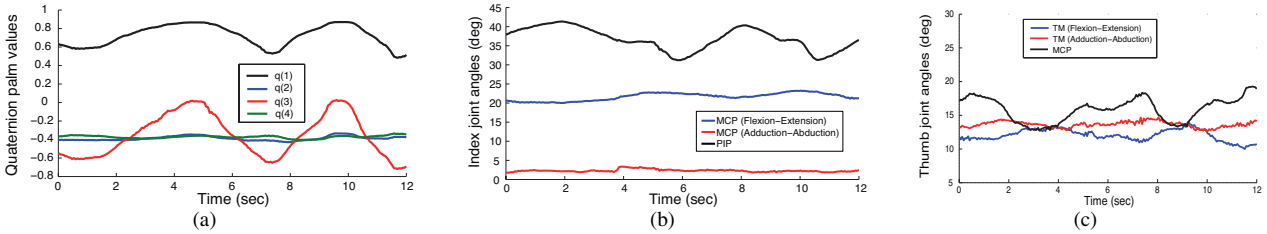

(a) (b) (c)

Fig. 7. Experiment 3: the user was asked to gently grasp a light object and freely rotate the palm maintaining the hand configuration with switched-off wearable haptic devices. (a) Quaternion of the palm during the motion. (b) Joint angles of the index finger. (c) Joint angles of the thumb.

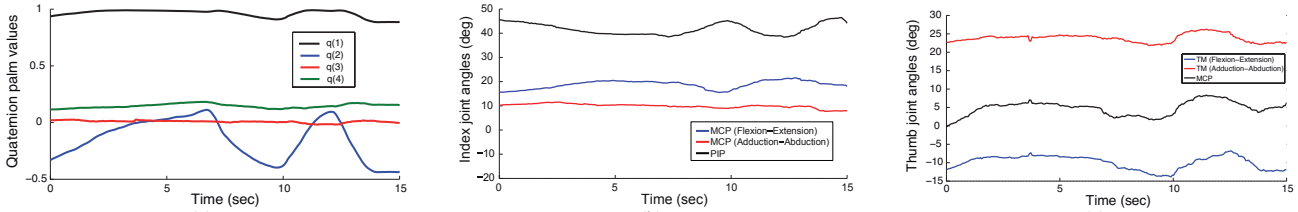

(a) (b) (c)

Fig. 8. Experiment 3: the user was asked to gently grasp a light object and freely rotate the palm maintaining the hand configuration with switched-on wearable haptic devices (the devices generated the maximum force). (a) Quaternion of the palm during the motion. (b) Joint angles of the index finger. (c) Joint angles of the thumb.

[23] L. Meli, C. Pacchierotti, and D. Prattichizzo. Sensory subtraction in robot-assisted surgery: fingertip skin deformation feedback to ensure safety and improve transparency in bimanual haptic interaction. *IEEE Trans. on Biomedical Engineering*, 61(4):1318–1327, 2014.

[24] D. Roetenberg, H. J. Luinge, C. T. M. Baten, and P. H. Veltink. Compensation of magnetic disturbances improves inertial and magnetic sensing of human body segment orientation. *IEEE Trans. on Neural Systems and Rehabilitation Engineering*, 13:395–405, 2005.